Type of contribution:
Editorial
▶ Research Paper
Case Study
Review Paper
Scientific Data
Report of Tech. Application

e-issn. 2798-5245

Mechanical Engineering for Society and Industry
Vol. 4, No. 1 (2024) pp 92-102
https://doi.org/10.31603/mesi.10799

Impact of morphological and mechanical components on inconel 625 grinding using common cylindrical grinding wheels

Manivannan Ramamoorthy[1], Vairavel Madeshwaren[2]*, Suresh Thangavel[3], Thangaraj Rajpradeesh[4]

[1] Department of Mechanical Engineering, Muthyammal Engineering College (Autonomous), Salem, Tamil Nadu 637408, **India**
[2] Department of Mechanical Engineering, Annapoorna Engineering College, Salem, Tamil Nadu 636308, **India**
[3] Department of Mechanical Engineering, Kumaraguru College of Technology, Coimbatore, Tamil Nadu 641049, **India**
[4] Department of Mechanical Engineering, Kalasalingam Academy of Research and Education, Krishnankoil, Tamil Nadu 626126, **India**
✉ phdannauniv2020@gmail.com

This article contributes to:

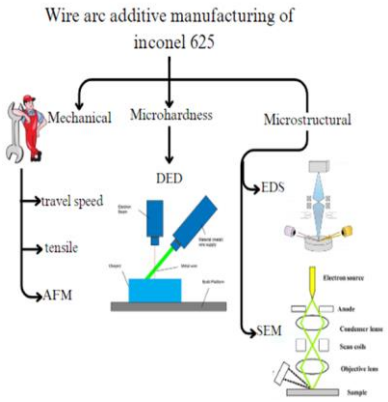

Highlights:

- This research thoroughly examines the microstructure of Inconel 625 walls made using milling techniques based on Gas Tungsten Arc Welding (GTAW).
- The walls constructed with a circular weave design demonstrated superior performance to a stringer bead design.
- Fracture zones were analyzed using scanning electron microscopy (SEM) and energy dispersive spectroscopy (EDS), revealing ductile fracture modes dominated by Ni and Cr, with traces of Nb and Mo.

Abstract

This study used a grinding technique based on Gas Tungsten Arc Welding (GTAW) to create walls composed of Inconel 625 alloy. Mechanical and microstructural (MM) adjustments are structural and mechanical alterations that take place during the additive manufacturing process of Inconel 625 grinding. A thorough examination of the modifications made to the nickel superalloy Inconel 625's (I-625) microstructure was conducted during the grinding process. A circular weave and a stringer bead design were used to construct the wall. Tensile properties and microstructural analyses were assessed for each wall. Using scanning electron microscopy (SEM) and energy dispersive spectroscopy (EDS), the fracture zones of the tensile specimens were examined. The microstructure is mostly composed of equiaxed dendrites, although a unique combination of discontinuous and continuous cellular dendrites can be observed along the cross-section. In tensile testing, circular woven walls performed better than stringer bead walls. The EDS and AFM results show that Ni and Cr make up the majority of the fracture zone, with traces of Nb and Mo. Because there are no lave phases, the fracture mode is ductile. The elemental mapping, which shows the homogenous dispersion of Ni and Cr inside the fracture zone, provides additional evidence in favor of the ductile failure mode. The UTS of the time-consuming TS samples is somewhat higher and exhibits a steadily rising bias in comparison to the specimens with quick TS. The highest level of the UTS sample is 10 %.

Keywords: Inconel 625; Grinding process; Scanning Electron Microscope; Tensile; Travel speed

Article info
Submitted: 2024-02-07
Revised: 2024-04-03
Accepted: 2024-04-25

Publisher
Universitas Muhammadiyah Magelang

1. Introduction

Additive Manufacturing (AM) is a potential process for creating large, complex-geometry, entirely dense metal objects. AM uses a construction technique called layer-by-layer building [1].

Nomenclature			
GTAM	: Gas Tungsten Arc Welding	AM	: Additive Manufacturing
DED	: Direct Energy Deposition	MH	: Micro-Hardness
EDS	: Energy Dispersive Spectroscopy	AFM	: Abrasive Flow Machining
SEM	: Scanning Electron Microscopy	OM	: Optical Microscope
WLAM	: Wire and Laser Additive Manufacturing	WEDM	: Wire Electric Discharge Machine
GMAW	: Gas Metal Arc Welding	WFS	: The Wire Feed speed
BTF	: Buy to Fly		

In the wire-based process, wire is melted rather than powder to create metal components using a laser, electron beam, or electric arc. [2]. A potential application for AM machinery is grinding, which uses an electric arc and wire as a deposition medium to create things [3]. Compared to other metal AM technologies, grinding processes require a higher high-temperature effort and lower cooling rates. This is beneficial for most materials that are advertised for sale. Researchers refer to all wire-based AM processes that use arc welding as a group as [4].

Recently, grinding processes have become more popular than AM processes where the starting raw material is alloy powder [5]. This is due to the fact that it has two main causes. The comparatively high price of metal powders, especially alloy powders, is the first of these issues [6]. The second justification for adopting wire feed systems is the ability of the grinding process in particular to produce extraordinarily large metallic parts at a low cost and at a rapid production rate [7]. In addition, the process is environmentally friendly due to its high material utilization, low equipment costs, and other advantages. As a result, wire feed systems—in particular, grinding processes—have begun to garner increasing attention from the industrial sector worldwide in recent years. Apart from its superior deposition rate in comparison to other additive manufacturing methods like laser-based AM processes [8], the technology is primarily optimized for the cost-effective production of large components. The grinding method has been more popular in several industries due to its adaptability and ability to produce complex mechanisms at high declaration rates [9]. It is particularly well-suited to producing large metal components. grinding offers advantages for cost-saving and material utilization in addition to its versatility. It also exhibits energy and material consumption efficiency [10]. With lower tool costs and a lower Buy to Fly (BTF) ratio than traditional methods, grinding makes large component manufacturing more affordable. With its increased creep strength, good weldability, and tensile strength, I-625 is a super alloy based on nickel that is primarily utilized in heavy temp. and corrosion applications in the aerospace, marine, and defense industries [11], [12]. The material's exceptional tensile strength is a result of the solid-solutioning action of the refractory alloying elements molybdenum and niobium [13]. At the moment, the production and repair of high-value components use Inconel 625 alloy parts more and more. Over the past few years, the automotive and aerospace sectors have grown significantly, which has made the use of better and lighter components necessary. Because of their complexity, the components are typically difficult to create using traditional manufacturing methods because they require a lot of machining and related procedures. With the advancement of AM technologies, intricate components may now be produced or repaired affordably. AM, also referred to as 3D printing, builds a component layer by layer [14]. The rapid development of additive manufacturing (AM) technologies across several industries has been facilitated by their capacity to decrease material waste, enhance design flexibility, offer high degrees of customization, and employ a diverse range of materials such as metals, composites, and polymers [15]. The manufacturing of I-625 alloy using grinding was investigated in this work. This incentive could improve the grinding processes that are used to produce I-625 alloys. The grinding process is used in the production of UTS, which results in components with mechanical properties better than those of traditionally cast I-625 alloy parts. To keep costs down, the study looks into how well Inconel 625 (IN 625) grinds while utilizing silicon carbide and alumina traditional grinding wheels. The outcomes demonstrate that the alumina wheel works better at a deeper cut and is more appropriate for grinding IN 625 [16]. Because grinding offers excellent tolerances and a polished surface finish, it is the most cost-effective method of machining difficult materials like nickel-based superalloys. However, because of their poor heat transmission, high-temperature aerospace components frequently result in thermal issues. To reduce thermal damage and residual stress, methods for detecting grinding temperature and fine-tuning grinding settings are covered in this study [17]. Using machine learning and response surface approach, the study investigates the grinding performance of Inconel 625. Lower tangential forces and improved ground surface quality, according to the results, validate MQL grinding as a sustainable substitute. This is corroborated by chip morphology results and micro-graph studies [18].

Using response surface methods and machine learning approaches, the study investigates the grinding performance of Inconel 625. Findings suggest MQL grinding as a viable substitute by demonstrating reduced tangential forces and improved ground surface quality. This is supported by results from chip morphology studies and micro-graph inquiries [19]. Because of its resistance to creep and high temperatures, INCONEL® superalloys, a type of nickel-based alloy, are being employed more and more in industries including energy power plants and the automobile industry. But because of their poor work hardening and low heat conductivity, these alloys are challenging to cut, which can lead to early tool wear and subpar final product finishing. The objective of this study is to provide an overview and analysis of the advancements made in INCONEL® machining during the last five years, together with current solutions and research viewpoints. Traditional cutting tool technology has advanced, but because of the inherent qualities of INCONEL® 718 and 625, machining them continues to be a major difficulty [20]. Using a porous metal-bonded cubic boron nitride super abrasive wheel, the study examined high-efficiency deep grinding of Inconel 718 nickel-based superalloy. Long-term maintenance of a low grinding temperature and energy partitioning between 2% and 6% were seen in the results. Excellent performance was aided by having enough space for chips and coolants in storage. The two most common wear patterns were abrasion wear and grain fracture, with chips loading and grain pullout being important factors [21].

Machinability issues with thermoresistant superalloys require novel manufacturing techniques. A solution called super abrasive machining (SAM) is suggested, which combines milling feed rates and grinding tools. The viability of roughing operations in Inconel® 718 is assessed in this paper, demonstrating flank SAM is an appropriate and manageable method for enhancing the white layer, residual stresses, microhardness, and roughness of nickel-based superalloy components [22]. Utilizing High Velocity Oxygen Fuel (HVOF) to manufacture AISI 4140 steel plates and characterizing them with metallography, roughness measures, and X-ray diffraction, the study assessed the corrosion resistance of Inconel 625 coatings on these plates. The coatings' performance was significantly impacted by surface finishing, according to the results [23].

The approach for fuzzy logic-based sequential grinding process optimization is presented in this research. It focuses on establishing goals and limitations for the machining process while taking the order of operations and dimensional and shape errors into account [24]. The purpose of this work is to fabricate functionally graded coatings utilizing titanium carbide and iron powders in order to improve metal matrix composite coatings. Fe particles reduced in weight proportion whereas TiC particulates grew from 25% to 100%. A coating system consisting of a single layer of titanium carbide coating, a bond coat of NiCrAlY, and a topcoat of 100% TiC was created. Mechanical characteristics, scanning electron microscopy, and X-ray diffraction were assessed. Higher wear resistance and adhesion were displayed by the FGC sample [25]. In this investigation, four MMC specimens with various reinforcements were created using the stir casting process. These specimens' mechanical qualities were examined, and their features were visually displayed [26]. The goal of the project is to enhance the wear resistance and surface micro-hardness of SAE 420 steel by the optimization of low-power laser hardening process parameters, specifically for dry sliding applications in biomedical industries. According to the results, the surface micro-hardness of the treated samples varies, and they have a higher wear resistance than the untreated samples. Significant improvements in material removal patterns are revealed when the study compares the results of the dry sliding wear test with samples that were not treated [27].

The main objective of this study is to examine the grinding process of I-625 alloy, revealing MM alterations in the material's physical characteristics and internal framework. Additionally, the main purpose of this article is to analyze the Mechanical and morphological components o n the grinding of Inconel 625 with CGW.

2. Methods

The main goal is to produce I-625 using the grinding wheel process. A detailed analysis is done on the grinding wheel on I-625, including its MM features. Furthermore, an analysis and comparison were conducted between the MM characteristics of the 3 fabricated specimens produced by the grinding process and those of I-625 alloy formed through casting. It is demonstrated that the grinding works well for producing I-625 alloys. For the welding trials, the Fronius GTAW Advanced 4000R power source was combined with a gas shielding system, wire feeding system, computer control system, and water-cooling system to form the grinding system. Q235 steel was employed

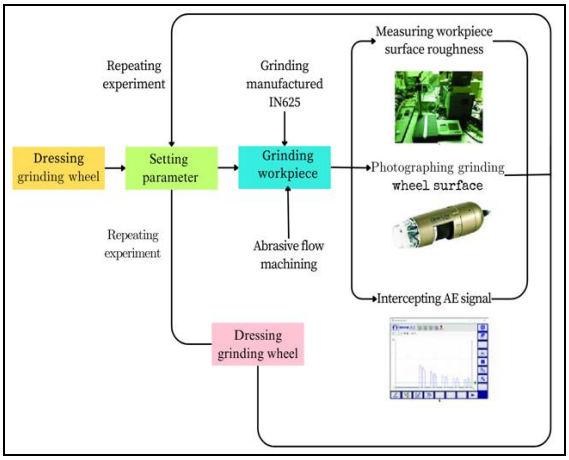

Figure 1. Flowchart of the proposed methodology

Table 1. The weight percentage of Inconel 625 wire's chemical composition

Element	Content
Al	≤ 0.4
C	≤ 0.3
Cr	20–25
Fe	≤ 5.5
Mn	≤ 0.9
Mo	9–12
Nb	3.19–4.18
Ni	Balance
Ti	≤ 0.4

as foundation metal, with parameters of width, thickness, and length. In the tests, Inconel 625 wire was typically composed of the components shown in **Table 1**. **Figure 1** shows the architecture of the proposed methodology.

Figure 2 depicts the welding experiment in representation. Prior to fixing the wire on the layer applied in the previous pass, the wire in the grinding was heated. Each layer was vertically placed perpendicular to the formerly formed layer to minimise fractures, porosity, and improve the development of the deposited layer. The layer's size varied greatly because of the layer remelting and rapid heat buildup generated by continuous deposition. To avoid this problem and guarantee the quality of the sample, a technique known as inter-pass cooling was employed. The way the inter-pass cooling technology was implemented caused the temperatures of the layer underneath it to drop to 400 °C.

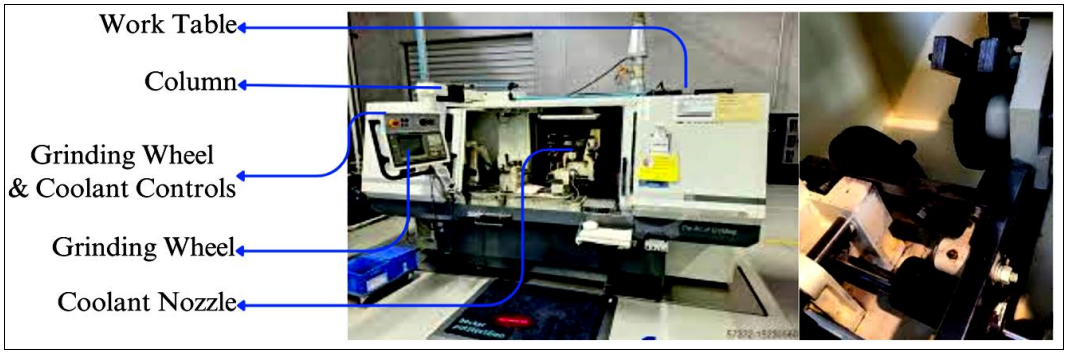

Figure 2. CNC cylindrical grinding device

An atmosphere of heliumargon gas, consisting of 35% helium and 75% argon, was kept in place during the operation at a flow rate of 17 litres per minute to keep the molten metal pool from oxidising. Side view of the grinding manufactured IN625 are provided in **Figure 3**.

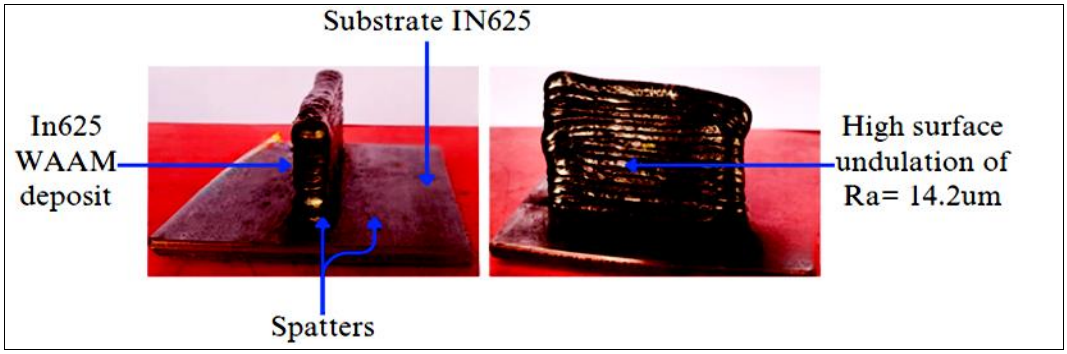

Figure 3. Grinding manufactured IN625 is shown in (a) front view and (b) side view

2.1. Mechanical Analysis

The specimen typically resembles a little rod or wire and has a thin, cylindrical form. It is meticulously constructed layer by layer using the grinding method, which involves precisely melting and depositing a wire electrode. By subjecting this test sample to axial forces during testing as a typical sample of the griding-produced component, experts are able to evaluate its elongation, tensile strength, and other crucial mechanical properties. **Figure 4** shows the grinding process. Each specimen underwent a grinding additively manufactured Inconel 625 for machi-

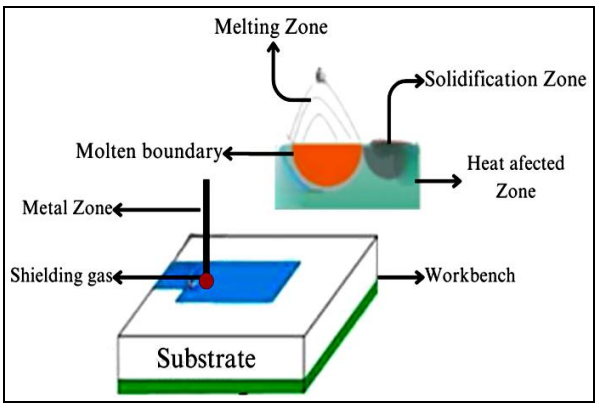

Figure 4. An illustration of the grinding process

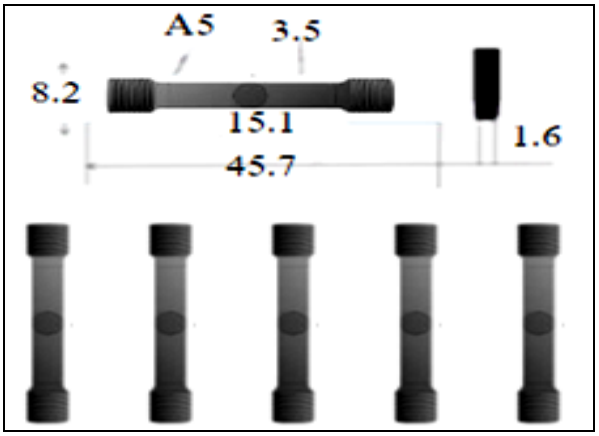

Figure 5. The process for designing tensile test specimens

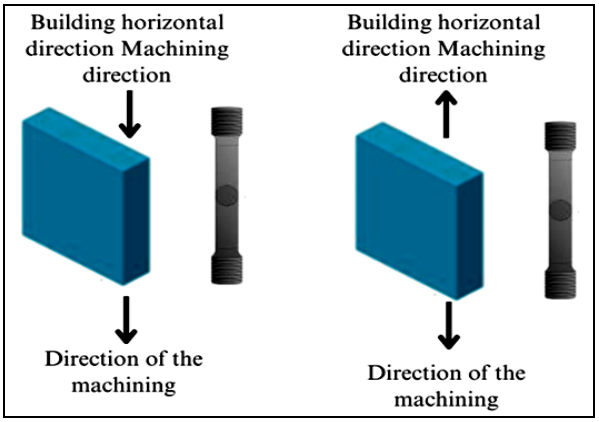

Figure 6. Diagrammatic depiction of the intercept's orientation of the tensile sample

ning, and then it was polished and ground in preparation for the testing procedure to ascertain its mechanical properties. The strength and strength of the deposits could be assessed thanks to the way the tensile tests were conducted. The test materials that underwent grinding processing are schematically depicted in **Figure 5** and **Figure 6**. The specimens undergoing microstructure examination underwent ultrasonical cleaning.

Tensile specimens for testing were created from the machined wall using grinding process in accordance with ASTM-E8. The specimens were sliced perpendicular to the vertical direction of weld as well as horizontally along the direction of weld. To guarantee precise measurement of the tensile characteristics, three samples were collected for each of the walls, one in each direction. A universal tensile testing device with the following parameters was used to load and stress all twelve samples to the point of failure while they were evaluated at room temperature. 25 kN maximum force at full velocity, 0.01 kN resolution, and a load capacity of 5–50 kN. There had a 0.005 to 500 mm/min speed range. The device featured a function that allowed for simultaneous monitoring of applied tension and elongation. After the samples had been loaded at a constant strain rate, genuine strain and stress curves were generated. The locations of the tensile samples taken out of the fake walls are depicted in **Figure 5**.

2.2. Abrasive Flow Machining (AFM)

Through the enhanced quality of the nozzle traits, AFM may be utilised to treat injector nozzles to improve engine efficiency and emissions. The method of abrasive flow machining yields a variety of consistent, repeatable outcomes. A concentration of abrasive granules and a flexible semisolid carrier make up the process media. AFM (**Figure 7**) is a useful technique for eliminating the grinding - produced recast layer. However, when an intricate hole is polished using this method, the surface roughness will not be consistent. Their suggested technique shows that the flow characteristics of the medium in AFM and shear forces throughout the polishing process are key factors in regulating the roughness throughout the surface.

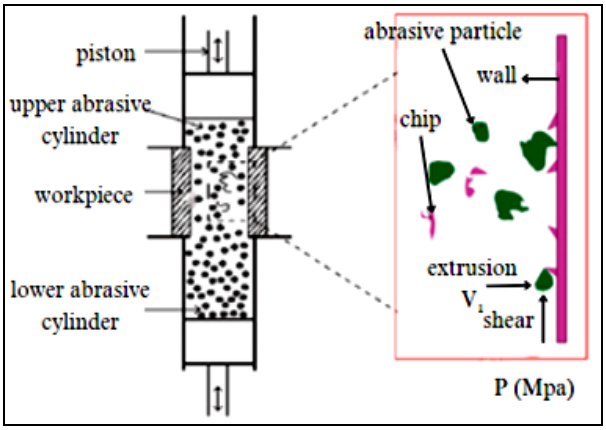

Figure 7. AFM structure

2.3. Microstructural Analysis

The test findings reflect the anisotropic nature of the material by placing the specimen's axis parallel to the path of deposition. This reflects the deformation and strength characteristics of the material as they occur in actual grinding -built components. The microscopic architecture of the samples is being examined using three distinct kinds of microscopes: an EDS, an Optical Microscope (OM), and a SEM. One millimeter is loaded every minute throughout the tensile test procedures. The tensile specimen's fracture surface geometries were ascertained by SEM analysis, and the elements' magnitude at the specimen's fracture location was ascertained by EDS. To ascertain the principal element dispersion in the broken region of the tensile sample, an element mapping investigation was performed. The specimen's microhardness value (MH) was determined using a Wilson Wolpert Vicker microhardness tester over the whole wall's cross-section. For the loading condition, the specimen was subjected to a 200 g weight, and a 10-second dwell time was allowed.

3. Results

3.1. Results of Mechanical Properties

In comparison to casting-made specimens, grinding specimens exhibited better tensile and percentage elongation values, along with a little UTS advantage. The outcome is a dimple as big as the result caused by the grains getting coarser and the alloying elements separating. Grain coarsening and the likelihood of precipitate phases occurring are both increased by slower transit speeds. Thus, the microstructure, precipitate stages, and strengthening elements in the solid solution all significantly affect the tensile properties.

3.2. Ultimate Tensile Strength

UTS plays a major role in evaluating the mechanical properties of components manufactured after the grinding process. Achieving the desired UTS is essential since it directly affects the structural integrity and load-bearing capacity of the manufactured components. Usually, UTS measured by newtons per square meter (N/m^2). Manufacturers can tailor the UTS-produced parts to meet specific requirements by selecting process parameters such as deposition rate, material composition, and layer height with care.

3.3. Travel Speed

When determining the efficacy and calibre of the additive process, the TS is essential. The term "travel speed" refers to the rate at which the flame of a welding or deposition device moves along the prearranged path as it deposits material layer by layer.

3.4. Elongation

Elongation is a crucial mechanical property that is very important in grinding process. With the innovative AM technique, a metal structure is assembled layer by layer using an electric arc. **Table 2** shows the results of UTS, TS and Elongation with different samples.

Table 2. Result of UTS, TS, and Elongation in different process samples

Samples	Ultimate tensile strength (N/m^2)	Travel speed	Elongation
Sample 1	653.9	11.45	52.67
Sample 2	683.67	12.45	55.45
Sample 3	392.56	13.45	56.56

3.5. Results of Micro-Hardness (MH)

Table 3. Impact of different longitudinal section elevations in the specimen on the micro-hardness

Distance from the interface (mm)	Micro-hardness (HV)
2	165
4	255
6	254
8	240
10	245
12	245
14	259
16	253
18	244
20	242
22	270

As build height increases, the MH demonstrates how the MH changes. MH is, on average, 264.4 HV next to the substrate region. Growing in height, the microhardness eventually reaches around 255.2 HV. Average MH in the higher area is 246 HV. With a typical hardness of about 259.5 HV, the layer that was placed down last was nonetheless. This is supported by the fact that the MHvalue is high and the crystals in the bottom layer and final layers are fine (**Table 3**).

3.6. The Grinding Deposition's Torch TS and Voltage

Table 4. TorchTS and grinding deposition voltage numerical results

	Values	
	Torch	Voltage
Sample 1	10.7	28.4
Sample 2	11.34	28.5
Sample 3	13.3	28.7

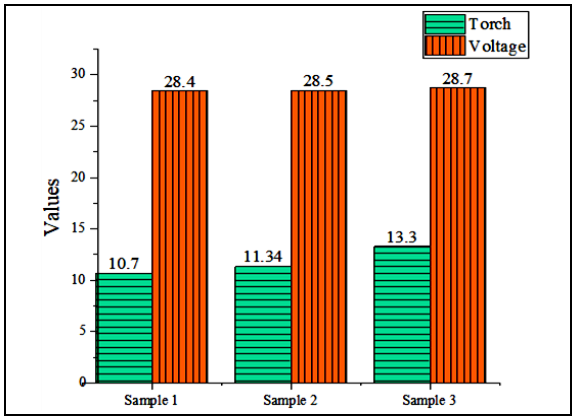

Figure 8. The voltage of the grinding deposition and torch TS

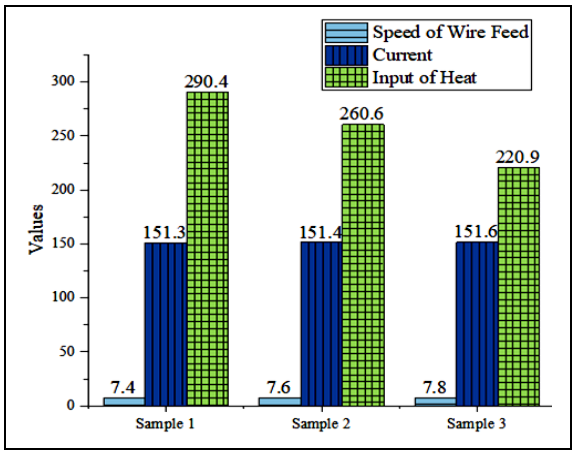

Figure 9. Grinding deposition's current, heat input, and WFS

The welding torch's speed along the workpiece is determined by the Torch TS value, which ranges from 8.5 to 10.2. This in turn impacts the material's distribution and the rate at which layers are deposited. To maintain total control over the heat flow and accomplish precise layer alignment, this speed must be changed. The potential difference between the electrode's surface and the object being worked on is controlled by voltage, a crucial electrical parameter. This variation directly affects the reliability of the arc, its heat output, and its penetration depth (**Table 4** and **Figure 8**).

The grinding deposition's WFS and input of heat and current The WFS regulates the pace at which the metal wire is introduced, directly influencing the speed and distribution of the material throughout the deposition process. An essential electrical parameter that influences fusion and metallurgical properties, current regulates the strength of the arc, and, in turn, the heat generated. The heat input, which is the outcome of the current and wire feed rate, determines the total thermal energy of the material. Grain structure, residual stresses, and cooling rate are just a few of the characteristics that are greatly impacted by this thermal energy (**Table 5** and **Figure 9**).

Table 5. The numerical results of the grinding deposition's current, heat input, and WFS

Samples	Values		
	Speed of Wire Feed	Current	Input of Heat
Sample 1	7.4	151.3	290.4
Sample 2	7.6	151.4	260.6
Sample 3	7.8	151.6	220.9

3.7. Microstructure (SEM)

The optical micrographs show every longitudinal segment of the specimen that was deposited under different circumstances. Sixteen layers are deposited, each measuring 3.6 mm in height, to produce a layered appearance. None of the deposited samples showed any defects, like holes in the deposit or inter-layer fissures between the substrate and base layer. Most of the time, the direction of heat flow dictates which way grains develop; grains preferentially develop in the opposite way of the largest temperature gradient. If the substrate does not cool the melt pool in any way, the crystal will grow vertically. The direction of grain growth does not, however, precisely line up with the liquid - solid border. During the CNC AM process, these previously produced base layers serve as the primary cooling components. To ascertain the manner of failure, SEM examination was performed on the fracture surface. It was discovered that every specimen lacked internal flaws like inclusions and pores. On the other hand, tensile test specimens' cracked surfaces showed voids and dimples, indicating a ductile failure mode. In comparison to vertical specimens, the dimples on walls "A" and "B" are bigger for horizontal samples. The horizontal samples exhibit dimples that are dispersed throughout the region rather than focused in a single area. As seen in **Figure 10** in contrast, the dimples in vertical samples are uniformly spaced apart and likewise localised in certain locations.

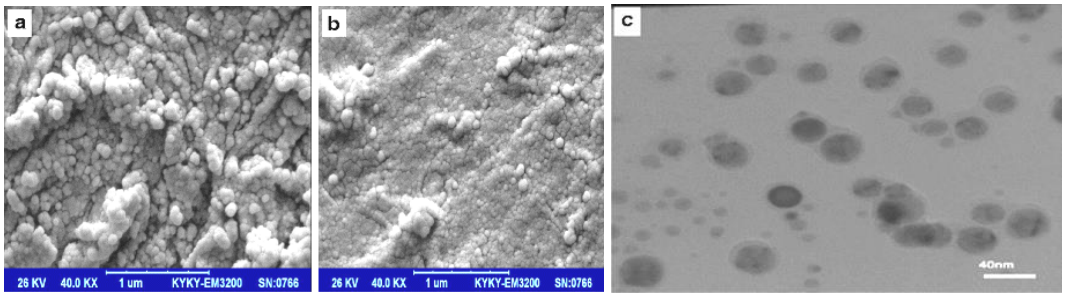

Figure 10. SEM images

4. Discussion

4.1. Mechanical Properties

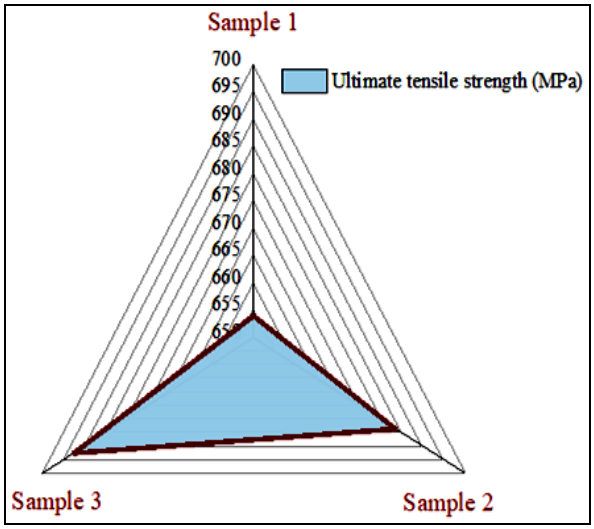

Figure 11. Different method of processing I-625 for TP of UTS

Comparable to the specimens with quick TS, the UTS of the time-consuming TS samples is slightly higher and shows a gradually increasing bias. Because the presence of small grains can greatly improve mechanical properties, this disparity is a result of the various microstructures (**Figure 11**). **Figure 12** show the casting elements for comparison together with the tensile properties of every sample deposited with a range of TS. **Figure 13** percentage elongation findings indicate that the TP of the specimen deposit can be increased without elongation falling between 43.5 to 46.6%.

4.2. SEM Analysis

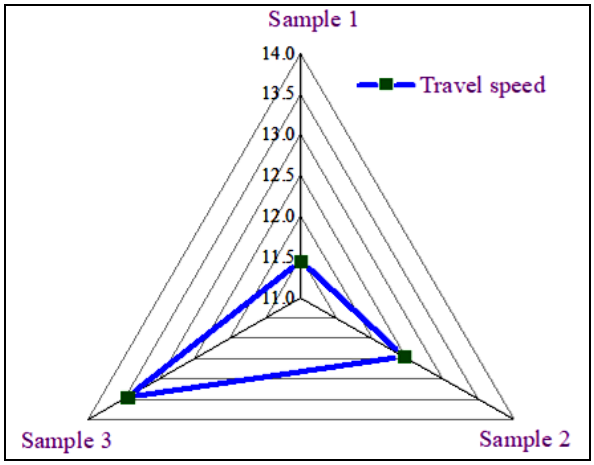

Figure 12. Different processing of I-625 by TP of TS

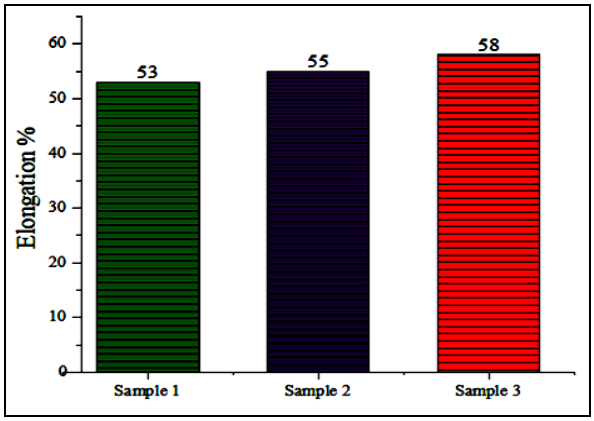

Figure 13. I-625 processing using a different TP of Elongation method

The lowest and highest UTS samples underwent EDS analysis to ascertain the existence of lave stage and to examine the chemical makeup of the fracture zone. **Figure 14** display both samples' chemical compositions. The specimen's fracture location was the site of the EDS analysis. To determine the precise size of the key elements, present in the location, a scan was conducted. **Figure 14a** illustrates that Ni and Cr account for the majority of the contribution, which is 76% in the case of other elements. Additionally, the highest UTS sample had the components in roughly 86% of cases. The failure mechanism is strengthened to be as ductile as possible by the high percentage of Ni and Cr present. Furthermore, in the lowest and highest UTS samples, respectively, the level of Mois is approximately 6%, 10%, and Nb is approximately 4%, 7%. This rules out the existence of the laves phase, which would only exist if both components made up one-third of the composition overall.

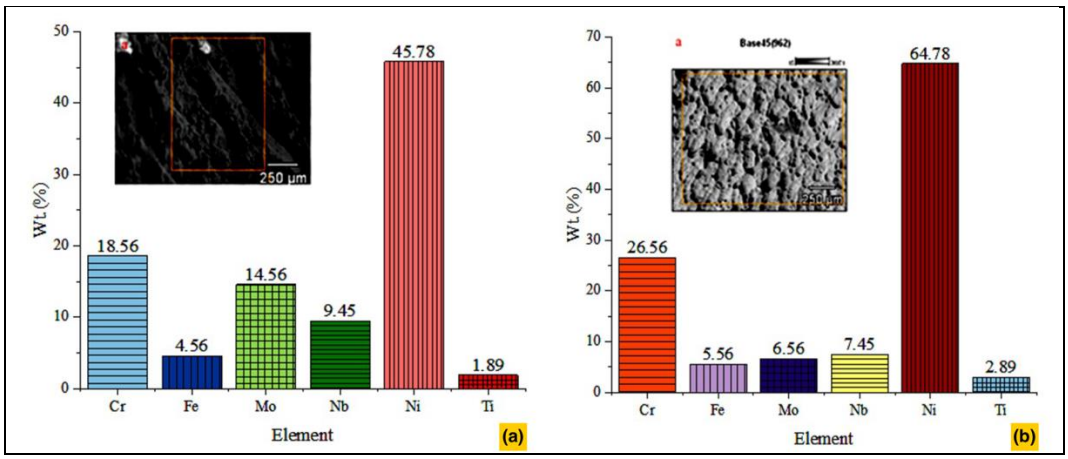

Figure 14.
(a) The lowest UTS specimen's EDS;
(b) The highest UTS specimen's EDS

5. Conclusion

The study used to grind to generate the I-625 alloy, revealing the impact of TS on its physical characteristics and internal framework. The resulting MM features were examined under a microscope, revealing different microstructures. The lower layers contained fine primary cellular arrangements, while the final layer had a structure-like appearance. As one moved away from the interface, the primary structure transformed into a columnar dendrite with distinctive secondary dendritic arms. This change was caused by the presence of the precipitate phase and a decrease in the solid state of the reinforcing element due to the alloy's microstructure. However, the rapid cooling and heating cycles could potentially compromise the integrity of structures and dimensional accuracy. Further research could enhance our understanding of grinding's potential and aid in producing robust, high-performing components for various industrial applications.

Limitations

Inconel 625 has a low thermal conductivity, grinding it is a challenging procedure. The machining tool itself suffers from insufficient heat dissipation from the machining zone, which shortens its lifespan. As a result, the workpiece develops dimensions and shape errors.

Authors' Declaration

Authors' contributions and responsibilities - The authors made substantial contributions to the conception and design of the study. The authors took responsibility for data analysis, interpretation, and discussion of results. The authors read and approved the final manuscript.

Funding – This research study is sponsored by the institution's name. Thank you to this college for supporting this article.

Availability of data and materials - All data is available from the authors.

Competing interests - The authors declare no competing interest.

Additional information – No additional information from the authors.

References

[1] W. Yangfan, C. Xizhang, and S. Chuanchu, "Microstructure and mechanical properties of Inconel 625 fabricated by wire-arc additive manufacturing," *Surface and Coatings Technology*, vol. 374, pp. 116–123, Sep. 2019, doi: 10.1016/j.surfcoat.2019.05.079.

[2] A. Chintala, M. Tejaswi Kumar, M. Sathishkumar, N. Arivazhagan, and M. Manikandan, "Technology Development for Producing Inconel 625 in Aerospace Application Using Wire Arc Additive Manufacturing Process," *Journal of Materials Engineering and Performance*, vol. 30, no. 7, pp. 5333–5341, Jul. 2021, doi: 10.1007/s11665-021-05781-6.

[3] A. Safarzade, M. Sharifitabar, and M. Shafiee Afarani, "Effects of heat treatment on microstructure and mechanical properties of Inconel 625 alloy fabricated by wire arc additive manufacturing process," *Transactions of Nonferrous Metals Society of China*, vol. 30, no. 11,

pp. 3016–3030, Nov. 2020, doi: 10.1016/S1003-6326(20)65439-5.
[4] Y. Wang *et al.*, "Effect of magnetic Field on the microstructure and mechanical properties of inconel 625 superalloy fabricated by wire arc additive manufacturing," *Journal of Manufacturing Processes*, vol. 64, pp. 10–19, Apr. 2021, doi: 10.1016/j.jmapro.2021.01.008.
[5] M. Cheepu, C. I. Lee, and S. M. Cho, "Microstructural Characteristics of Wire Arc Additive Manufacturing with Inconel 625 by Super-TIG Welding," *Transactions of the Indian Institute of Metals*, vol. 73, no. 6, pp. 1475–1479, Jun. 2020, doi: 10.1007/s12666-020-01915-x.
[6] D. Sarathchandra and M. Davidson, "Effect of heat input on mechanical and microstructural properties of Inconel 625 depositions processed in wire arc additive manufacturing," *Proceedings of the Institution of Mechanical Engineers, Part E: Journal of Process Mechanical Engineering*, vol. 235, no. 5, pp. 1439–1448, Oct. 2021, doi: 10.1177/09544089211004718.
[7] G. Ravi, N. Murugan, and R. Arulmani, "Microstructure and mechanical properties of Inconel-625 slab component fabricated by wire arc additive manufacturing," *Materials Science and Technology*, vol. 36, no. 16, pp. 1785–1795, Nov. 2020, doi: 10.1080/02670836.2020.1836737.
[8] S. Mohan Kumar *et al.*, "Microstructural Features and Mechanical Integrity of Wire Arc Additive Manufactured SS321/Inconel 625 Functionally Gradient Material," *Journal of Materials Engineering and Performance*, vol. 30, no. 8, pp. 5692–5703, Aug. 2021, doi: 10.1007/s11665-021-05617-3.
[9] M. Karmuhilan and S. Kumanan, "A Review on Additive Manufacturing Processes of Inconel 625," *Journal of Materials Engineering and Performance*, vol. 31, no. 4, pp. 2583–2592, Apr. 2022, doi: 10.1007/s11665-021-06427-3.
[10] M. Sharifitabar, S. Khorshahian, M. Shafiee Afarani, P. Kumar, and N. K. Jain, "High-temperature oxidation performance of Inconel 625 superalloy fabricated by wire arc additive manufacturing," *Corrosion Science*, vol. 197, p. 110087, Apr. 2022, doi: 10.1016/j.corsci.2022.110087.
[11] C. Zhang *et al.*, "On the Effect of Heat Input and Interpass Temperature on the Performance of Inconel 625 Alloy Deposited Using Wire Arc Additive Manufacturing–Cold Metal Transfer Process," *Metals*, vol. 12, no. 1, p. 46, Dec. 2021, doi: 10.3390/met12010046.
[12] T. A. Rodrigues *et al.*, "Wire and arc additive manufacturing of 316L stainless steel/Inconel 625 functionally graded material: development and characterization," *Journal of Materials Research and Technology*, vol. 21, pp. 237–251, Nov. 2022, doi: 10.1016/j.jmrt.2022.08.169.
[13] I. Jurić, I. Garašić, M. Bušić, and Z. Kožuh, "Influence of Shielding Gas Composition on Structure and Mechanical Properties of Wire and Arc Additive Manufactured Inconel 625," *JOM*, vol. 71, no. 2, pp. 703–708, Feb. 2019, doi: 10.1007/s11837-018-3151-2.
[14] A. Gamon *et al.*, "Microstructure and hardness comparison of as-built inconel 625 alloy following various additive manufacturing processes," *Results in Materials*, vol. 12, p. 100239, Dec. 2021, doi: 10.1016/j.rinma.2021.100239.
[15] V. Votruba *et al.*, "Experimental investigation of CMT discontinuous wire arc additive manufacturing of Inconel 625," *The International Journal of Advanced Manufacturing Technology*, vol. 122, no. 2, pp. 711–727, Sep. 2022, doi: 10.1007/s00170-022-09878-7.
[16] K. Kishore, M. K. Sinha, and S. R. Chauhan, "A comprehensive investigation of surface morphology during grinding of Inconel 625 using conventional grinding wheels," *Journal of Manufacturing Processes*, vol. 97, pp. 87–99, Jul. 2023, doi: 10.1016/j.jmapro.2023.04.053.
[17] S. N. Gupta and S. K. Chak, "Grinding temperature and its consequences on induced residual stresses during grinding of nickel-based superalloys: a review," *Engineering Research Express*, vol. 4, no. 4, p. 042002, Dec. 2022, doi: 10.1088/2631-8695/acaa1d.
[18] K. Kishore, S. R. Chauhan, and M. K. Sinha, "Application of machine learning techniques in environmentally benign surface grinding of Inconel 625," *Tribology International*, vol. 188, p. 108812, Oct. 2023, doi: 10.1016/j.triboint.2023.108812.
[19] L. Li *et al.*, "Mechanical behavior and modeling of grinding force: A comparative analysis," *Journal of Manufacturing Processes*, vol. 102, pp. 921–954, Sep. 2023, doi: 10.1016/j.jmapro.2023.07.074.
[20] A. F. V. Pedroso *et al.*, "A Comprehensive Review on the Conventional and Non-Conventional Machining and Tool-Wear Mechanisms of INCONEL®," *Metals*, vol. 13, no. 3, p. 585, Mar. 2023, doi: 10.3390/met13030585.
[21] Z. Li, W.-F. Ding, C.-Y. Ma, and J.-H. Xu, "Grinding temperature and wheel wear of porous metal-bonded cubic boron nitride superabrasive wheels in high-efficiency deep grinding," *Proceedings of the Institution of Mechanical Engineers, Part B: Journal of Engineering*

Manufacture, vol. 231, no. 11, pp. 1961–1971, Sep. 2017, doi: 10.1177/0954405415617928.
[22] H. González, O. Pereira, A. Fernández-Valdivielso, L. López de Lacalle, and A. Calleja, "Comparison of Flank Super Abrasive Machining vs. Flank Milling on Inconel® 718 Surfaces," *Materials*, vol. 11, no. 9, p. 1638, Sep. 2018, doi: 10.3390/ma11091638.
[23] M. S. de Lorenzi, R. M. Nunes, T. Falcade, and T. Clarke, "Evaluation of the Influence of Surface Finishing on the Corrosion Resistance of HVOF Applied Inconel 625 Coatings on Steel," *Materials Research*, vol. 21, no. 2, Dec. 2017, doi: 10.1590/1980-5373-mr-2016-0844.
[24] D. Lipiński, W. Kacalak, and B. Bałasz, "Optimization of sequential grinding process in a fuzzy environment using genetic algorithms," *Journal of the Brazilian Society of Mechanical Sciences and Engineering*, vol. 41, no. 2, p. 96, Feb. 2019, doi: 10.1007/s40430-019-1601-6.
[25] M. Rezapoor, M. Razavi, M. Zakeri, M. R. Rahimipour, and L. Nikzad, "Fabrication of functionally graded Fe-TiC wear resistant coating on CK45 steel substrate by plasma spray and evaluation of mechanical properties," *Ceramics International*, vol. 44, no. 18, pp. 22378–22386, Dec. 2018, doi: 10.1016/j.ceramint.2018.09.001.
[26] D. Bandhu, A. Thakur, R. Purohit, R. K. Verma, and K. Abhishek, "Characterization & evaluation of Al7075 MMCs reinforced with ceramic particulates and influence of age hardening on their tensile behavior," *Journal of Mechanical Science and Technology*, vol. 32, no. 7, pp. 3123–3128, Jul. 2018, doi: 10.1007/s12206-018-0615-9.
[27] S. V. Wagh *et al.*, "Effects of low-power laser hardening on the mechanical and metallurgical properties of biocompatible SAE 420 steel," *Journal of Materials Research and Technology*, vol. 30, pp. 1611–1619, May 2024, doi: 10.1016/j.jmrt.2024.03.153.